Inhibition of Calmodulin-Activated Smooth-Muscle Myosin Light-Chain Kinase by Calmodulin-Binding Peptides and Fluorescent (Phosphodiesterase-Activating) Calmodulin Derivatives†

Katalin Török,* David J. Cowley,‖ Birgit D. Brandmeier,§ Stephen Howell,§ Alastair Aitken,‡,§ and David R. Trentham§

School of Biological Sciences, Queen Mary and Westfield College, University of London, London E1 4NS, UK, and National Institute for Medical Research, Mill Hill, London, NW7 1AA, UK

Received November 11, 1997; Revised Manuscript Received January 27, 1998

ABSTRACT: Aspects of the biochemistry of calmodulin have been addressed that bear on its cell biological role as a mediator of Ca^{2+} regulation. Calmodulin-binding peptides derived from the amino acid sequence of smooth-muscle myosin light-chain kinase (MLCK) were characterized as inhibitors of calmodulin activation of MLCK-catalyzed phosphorylation of the smooth-muscle regulatory light chain (MLC). MLCK activity was determined by measuring the rate of formation of one of the reaction products, ADP, in a coupled enzymatic assay by continuous fluorimetric monitoring of NADH removal in 100 μM $CaCl_2$ at ionic strength 0.15 M, pH 7.0 and 21 °C. The K_m value of calmodulin was 3.5 nM, a value 16−35-fold greater than the K_d value of calmodulin for MLCK [Török, K., and Trentham D. R. (1994) *Biochemistry 33*, 12807−12820]. The different K_m and K_d values are most likely associated with the rate-limiting step in MLC phosphorylation being associated with product release from MLCK. The values of the inhibition constants, K_i, were the following: Ac-R-R-K-W-Q-K-T-G-H-A-V-R-A-I-G-R-L-$CONH_2$ (Trp peptide), 8.6 (±1.4 sd) pM; Y_4-analogue of Trp peptide (Tyr peptide), 7.3 (±0.1) nM; and A-R-R-K-W-Q-K-T-G-H-A-V-R-A-I-G-R-L-S-S (RS20-like peptide), 0.11−0.39 nM. The K_i values were consistent with kinetically determined K_d values of the peptides to calmodulin. Kinetic determination of K_d values required the use of a fluorescently labeled calmodulin, 2-chloro-(ϵ-amino-Lys_{75})-[6-(4-*N*,*N*-diethylamino-phenyl)-1,3,5-triazin-4-yl]-calmodulin (TA-calmodulin).[1] Since, as here, Lys_{75} is a convenient labeling site on calmodulin for the introduction of fluorescent probes, the biological activity of the Lys-modified calmodulins was evaluated. TA-calmodulin and calmodulin selectively modified by 1-*N*,*N*-dimethylaminonaphthalene-5-sulfonyl chloride (dansyl-C1) at Lys_{75} (dansyl-calmodulin) were characterized as activators of cyclic AMP phosphodiesterase (PDE) and inhibitors of MLCK. The K_m value for dansyl-calmodulin was equal to that of calmodulin, and that of TA-calmodulin was 3.5-fold greater. TA-calmodulin and Lys_{75}-labeled dansyl-calmodulin thus distinguish between PDE and MLCK being agonists to the former and antagonists to the latter.

Calmodulin is an intracellular Ca^{2+}-binding protein that in its Ca^{2+}-bound form binds to and activates a wide range of proteins and thereby regulates a variety of cellular processes (for review see *1*). Methods to probe cellular mechanisms in which calmodulin is implicated include the introduction of fluorescently modified calmodulin into cells to study its Ca^{2+} binding, cellular localization, or translational and rotational diffusion and to use target peptides to sequester calmodulin and hence inhibit calmodulin-dependent cellular processes. We have recently used the fluorescent protein TA-calmodulin and a high-affinity target peptide, Trp peptide (Ac-R-R-K-W-Q-K-T-G-H-A-V-R-A-I-G-R-L-$CONH_2$), to compare the activation kinetics of cytosolic and nuclear calmodulin, to visualize Ca^{2+}-activation-dependent and -independent localization of calmodulin, and to investigate the role of calmodulin in the control of mitotic transitions (*2*−*4*). Target peptides as inhibitors have proved useful in

† The work was supported by the National Institutes of Health Grant HLB 15835 to the Pennsylvania Muscle Institute and MRC, U.K.

* Corresponding author: School of Biological Sciences, Queen Mary and Westfield College, Mile End Road, London E1 4NS, UK. Tel: 44 171 775 3010. Fax: 44 181 983 0973. E-mail: k.torok@qmw.ac.uk.

‡ Present address: Department of Biochemistry, Hugh Robson Building, George Square, Edinburgh EH8 9XD.

§ National Institute for Medical Research.

‖ Present address: Synthelabo Biomoleculaire, 16, rue d'Ankara, 67080 Strasbourg Cedex, France.

[1] Abbreviations: AD, adenosine deaminase; AP, alkaline phosphatase; bis, *N*,*N*′-methylene-bis-acrylamide; cyclic-AMP, adenosine 3′,5′-cyclic monophosphate; dansyl-calmodulin, (ϵ-amino-Lys_{75})-(1-*N*,*N*-dimethylaminonaphthalene-5-sulfonyl)calmodulin; dansyl-Cl, 1-*N*,*N*-dimethylaminonaphthalene-5-sulfonyl chloride; DET-calmodulin, 2-chloro-(ϵ-amino-Lys_{75})-(6-*N*-ethylanilino-1,3,5-triazin-4-yl)calmodulin; DET-Cl, 2,4-dichloro-6-*N*-ethylanilino-1,3,5-triazine; DTT, 1,4-dithiothreitol; FAB, fast atom bombardment; F-moc, 9-fluorenylmethoxycarbonyl; LDH, lactate dehydrogenase; MES, 2-(*N*-morpholino)ethanesulfonic acid; MLC, regulatory myosin light chain from smooth muscle; MLCK, smooth-muscle myosin light-chain kinase; PDE, adenosine 3′,5′-cyclic monophosphate phosphodiesterase; PEP, phosphoenolpyruvate; PK, pyruvate kinase; PMSF, phenylmethylsulfonyl fluoride; SDS−PAGE, sodium dodecyl sulfate−polyacrylamide gel electrophoresis; TA-, 2-chloro-6-(4-*N*,*N*-diethylaminophenyl)-1,3,5-triazin-4-yl-; TA-calmodulin, 2-chloro-(ϵ-amino-Lys_{75})-[6-(4-*N*,*N*-diethylamino-phenyl)-1,3,5-triazin-4-yl]calmodulin; TA-Cl, 2,4-dichloro-6-(4-*N*,*N*-diethyl-aminophenyl)-1,3,5-triazine; TCA, trichloroacetic acid; TFA, trifluoroacetic acid.

S0006-2960(97)02773-6 CCC: $15.00
Published on Web 04/14/1998

establishing that Ca^{2+}-calmodulin is essential for cyclin degradation and exit from meiotic metaphase in *Xenopus* eggs (*5*) and in the regulation of the voltage-activated Ca^{2+} channels in smooth muscle (*6*−*8*). Fluorescently labeled calmodulins and inhibitor peptides have been used to monitor calmodulin activation by Ca^{2+} in living cells (*9*−*12*).

In this work we analyze aspects of the biochemistry that form the basis of the cellular processes. Thus the mechanism of calmodulin activation of MLCK relates to the use of peptides derived from the amino acid sequence of MLCK as probes of the cell biology of calmodulin. As indicated above, fluorescence labeling of calmodulin is an approach to monitoring the function of calmodulin in cells. The effect of fluorophores on the mechanism of the modified calmodulins' interactions with MLCK and other enzymes bears on the observed cell biology. These topics have been addressed through a series of kinetic studies on calmodulin and fluorescently labeled calmodulins together with some analysis of the site of fluorophore attachment.

When using target peptides for inhibitor studies of cellular processes, it is important to know, at least approximately, the K_d of the peptide and calmodulin under cellular conditions. The K_d of calmodulin and Trp peptide in the presence of Ca^{2+} is 6 pM (*13*), but these measurements were made using the isolated reagents in the absence of the relevant calmodulin-activated enzyme. We determined here whether the same K_d of Trp peptide for calmodulin was obtained in an assay that measured the inhibition of MLCK activity. This situation is closer to that encountered in cell biology, where inhibition by peptides presumably occurs through sequestering calmodulin from an enzyme such as MLCK. Accordingly, we have developed a continuous assay for MLCK activity that permits the determination of the relevant kinetic parameters, and so the competition between MLCK and target peptides for calmodulin can be measured.

The affinity of the Trp peptide for calmodulin (K_d = 6 pM) contrasts with the order(s) of magnitude lower affinity of other peptides related to the MLCK target peptide such as RS20 (*14*). It was important to understand the origin of this difference, so we have investigated the mechanism of an RS20-related peptide (kindly provided by Dr. M. Ikebe) interacting with TA-calmodulin. Furthermore, comparison of the K_m for calmodulin and the dissociation constant of calmodulin and MLCK in the presence of the substrates MLC and ATP, determined with the use of the peptide inhibitors, should lead to a greater understanding of the role of calmodulin in catalyzing MLCK activity.

The preparation of TA-calmodulin from TA-Cl and calmodulin indicated that Lys_{75} is the most reactive lysine in calmodulin (reviewed in *13*) and is therefore likely to be labeled extensively when calmodulin is treated with other amine-reactive fluorophores (*2, 3, 9, 19*). This prediction was tested by reacting calmodulin with dansyl-Cl. The resulting protein was examined for its specificity of labeling. A major fraction, dansyl-calmodulin, specifically labeled at Lys_{75}, was isolated. In addition, it is important to know the capacity of Lys_{75}-modified calmodulins to activate or inhibit calmodulin-dependent enzymes. By comparing the interactions of TA-calmodulin and dansyl-calmodulin with MLCK and PDE, the mechanisms of activation by calmodulin are shown to be distinct from one another.

MATERIALS AND METHODS

Protein and Peptide Preparation and characterization. Calmodulin was purified from pig brain, as described for bovine brain (*16*). TA-Cl was synthesized and characterized, and TA-calmodulin was prepared as described in ref *13*. Two batches of TA-Cl were used to label calmodulin with TA-Cl (Batch I) (*17*) containing 8.1% DET-Cl. Later work used TA-Cl (Batch II) (*18*) that was free of DET-Cl and was >99% pure by NMR. The contaminant, DET-Cl-labeled calmodulin, was spectroscopically silent at >330 nm and functionally indistinguishable from TA-calmodulin, and concentrations of TA-calmodulin made with TA-Cl (Batch I) were corrected for its presence. Dansyl-calmodulin was synthesized by reacting calmodulin and dansyl-Cl in the same conditions (pH 8.5 and 20 mM $CaCl_2$) as previously described for TA-calmodulin. Dansyl-calmodulin (2.5 mg) was purified to homogeneity (monitoring absorption at 215 nm) by reverse-phase HPLC on a Vydac 218TP54 C_{18} column (4.6 × 250 mm), and its protein properties were characterized. Dansyl-calmodulin is shown below to be distinct from the commercially available dansylated calmodulin (Sigma Chemical Co.), which showed several 215-nm absorption peaks in identical HPLC analysis.

MLCK was copurified with caldesmon from bovine rumen (*19*) by an extension of the procedure described for turkey gizzard (*20*). During purification, fractions containing MLCK were identified by activity assay (see below) and gradient SDS−PAGE (6.4−20% acrylamide:bis 30:1 containing 10% glycerol, Laemmli buffer system (*21*)). Differential identification of MLCK and caldesmon was facilitated by SDS−PAGE of heat-treated (2 min, 90 °C) aliquots of the relevant fractions, by which treatment caldesmon remained soluble whereas MLCK was precipitated. Caldesmon was identified by immunoblotting using antibodies specific to caldesmon (a gift from Dr. S. B. Marston) (*22*). Concentrated crude MLCK was supplemented with 1 mM DTT, 3 mM $MgCl_2$, 0.1 mM ATP, 0.1 mM PMSF, and 10% glycerol and rapidly frozen and stored at −80 °C in 2.5-mL aliquots. For further purification and the removal of caldesmon, aliquots were desalted on prepacked gel filtration columns (PD10, Pharmacia) and subjected to Mono Q FPLC (Pharmacia) as follows: a 200−600 mM linear gradient of NaCl (80-mL total volume) was applied in 20 mM Tris·HCl pH 7.5, 1 mM EGTA, 1 mM EDTA, 1 mM DTT, 3 mM $MgCl_2$, 0.1 mM ATP, and 0.1 mM PMSF to a Mono Q HR 10/10 column. Caldesmon typically eluted at 300 mM and MLCK at 370 mM NaCl. Homogeneous MLCK was obtained by rechromatography of 2.5-mL aliquots of the Mono Q MLCK pool desalted by PD10 filtration, on a 4-mL phosphocellulose column and with conservative pooling of the leading fractions. The MLCK was stored at −80 °C as above for crude MLCK. The final concentration of MLCK was 0.2−0.5 mg/mL. The yields were 0.6−1 mg of MLCK/200 g of rumen.

MLC was purified from the myofibrillar pellet of rumen after the extraction of MLCK: the myofibrils were homogenized at 4 °C in a Waring blender with 4 volumes of 10% TCA, 20 mM Tris·HCl pH 7.5, 1 mM EGTA, 1 mM EDTA, and 1 mM DTT. The homogenate was adjusted to pH 8.0, and it was allowed to stand at 4 °C for 1 h. The slurry was then centrifuged at 40000*g* for 20 min. The pellet was

Table 1: Peptide−Calmodulin Dissociation Constants[a]

		MLCK inhibition	equilibrium competition
		K_d (nM)	K_d (cal) (nM)
Trp peptide	*Ac*-R-R-K-W-Q-K-T-G-H-A-V-R-A-I-G-R-L-*CONH*$_2$	0.0086 (±0.0014)[b]	0.006 (±0.002)[c]
Tyr peptide	*Ac*-R-R-K- **Y**-Q-K-T-G-H-A-V-R-A-I-G-R-L-*CONH*$_2$	7.3 (±0.1)	5.5 (±1.7)[c]
RS20-like peptide	A-R-R-K-W-Q-K-T-G-H-A-V-R-A-I-G-R-L-S-S	0.11−0.39	0.09−0.64[d]
RS20	R-R-K-W-Q-K-T-G-H-A-V-R-A-I-G-R-L-S-S-S	1.6 (±0.3)[e]	nd[f]
control peptide	*Ac*-R-R-K-**E**-Q-K-T-G-H-A-V-R-A-I-G-R-**E**-*CONH*$_2$	nd[f]	4700[g]

[a] Residues typed in bold face are substitutions introduced into the chicken gizzard MLCK sequence. [b] Standard deviations. For the RS20-like peptide, extreme values of measurements are recorded. [c] Values published in ref *13*. [d] K_d for calmodulin was calculated from the kinetically determined K_d for TA-calmodulin on the basis that K_d for calmodulin is typically 0.4-fold that for TA-calmodulin. [e] Value published in ref *14*. [f] nd: not determined. [g] Aliquots of the control peptide were added to the standard solution (see Materials and Methods) containing 11 nM TA-calmodulin. TA fluorescence (λ_{ex} 365 nm, λ_{em} 415 nm) increased 1.7-fold on saturation with peptide. A K_d value of 11.8 μM was determined assuming 1:1 stoichiometry using Fortran program BINDPC (provided by E. P. Morris). A 0.4-fold K_d for TA-calmodulin gave the estimated K_d for calmodulin.

further processed essentially as described in ref *23*. Final purification of MLC was by Mono Q FPLC (HR 10/10) using a 0−1 M NaCl gradient in 20 mM Tris·HCl pH 7.5, 1 mM EGTA, 1 mM EDTA, and 1 mM DTT. MLC was identified by SDS−PAGE, then desalted and lyophilized. The yield was 80 mg of MLC/200 g of myofibrils.

Smooth-muscle MLC phosphatase (*24*) was a gift of Dr. D. Alessi and Professor P. Cohen.

The RS20-like peptide was a gift of Dr. M. Ikebe. The peptide was subjected to our routine analysis procedure: it was HPLC purified on a Vydac C_{18} column, and its mass by electrospray mass spectrometry was 2277 Da, confirming its structure (Table 1). The control peptide (Table 1) was synthesized by F-moc technology and purified to homogeneity by reverse-phase HPLC with a gradient (0.5% change/min) of 0.1% TFA in H_2O to 0.082% TFA in CH_3CN on a Waters Deltapak C_{18} column (30 mm × 30 cm) at a flow rate of 2 mL/min. Its molecular mass by electrospray mass spectrometry was 2032 Da, confirming its structure. Trp and Tyr peptides were characterized as in ref *13*.

Determination of Protein and Peptide Concentrations. A molar extinction coefficient (ϵ_0) of 3300 M^{-1} cm^{-1} at 275 nm was used for purified calmodulin in the absence of Ca^{2+} (*25*). The ϵ_0 value was 40100 M^{-1} cm^{-1} for TA-calmodulin in 1 mM EGTA, 100 mM KCl, 2 mM $MgCl_2$, and 50 mM K-MES at pH 7.0 and 21 °C as determined in ref *13*. The Bradford assay (*26*) was used to determine the protein concentrations of dansyl-calmodulin using unlabeled calmodulin as the standard. This led to the ϵ_0 value of 3400 M^{-1} cm^{-1} at λ_{max} = 335 nm measured in a solution of 1 mM EGTA, 100 mM KCl, 2 mM $MgCl_2$, and 50 mM K-MES at pH 7.0 and 21 °C (cf. ϵ_0 = 3400 M^{-1} cm^{-1} for the dansylated-calmodulin preparation described in ref *15*). We used the value ϵ_0 = 6740 M^{-1} cm^{-1} at 275 nm for MLC obtained for the turkey gizzard MLC (*23*). The calculated ϵ_0 for gizzard MLC is 4400 M^{-1} cm^{-1} (*27*), and thus the concentration estimates for MLC may be too small by a factor of 1.5. There is additional uncertainty with regard to the precision of MLC concentration measurements because bovine stomach MLC was used in this study. Furthermore MLC has a tendency to precipitate and to form a dimer through disulfide bond formation (B. Brandmeier, R. S. Ferguson, J. E. T. Corrie, J. Kendrick-Jones, and D. R. Trentham, unpublished work). Care is needed to avoid these problems, for example, by having DTT in the solution; otherwise MLC concentrations are lower than envisaged. Concentrations of MLCK and myosin phosphatase were determined by the Bradford assay with bovine serum albumin as the standard. Peptide concentrations were determined using ϵ_0 = 1400 M^{-1} cm^{-1} for the Tyr peptide and ϵ_0 = 5700 M^{-1} cm^{-1} at 278 nm for Trp and RS20-like peptides in aqueous solution at pH 7, and by weight for the control peptide (Table 1).

Identification of the Tryptic Peptides of Calmodulin as a Basis for Identifying Dansylated Peptides. Peptides obtained from a tryptic digestion of calmodulin were identified since their characterization was important for determining the labeling site(s) of dansyl-calmodulin. Individual peptides from the tryptic digests of calmodulin and dansyl-calmodulin were isolated by Vydac C_{18} HPLC and analyzed by FAB mass spectrometry. The sequence of elution of peptide peaks was the same as in ref *28* except that the relative position of peaks corresponding to the peptides of amino acids 1−13 and 14−30 was reversed. Only peaks in the vicinity of the dansylated peptides were analyzed. Thus peptides spanning 38−74 were not analyzed, but have been reported to elute after the ninth peak (residues 127−145) "peak 9" (*28*). Peak 9 appeared as a single peak in the elution profile obtained in ref *28*. In our elution profiles it always appeared as a broad or split peak. The C-terminal tryptic peptide of calmodulin might be expected to be 127−148 but is susceptible to anomalous tryptic cleavage including cleavage on the C-terminal side of Met_{145} (*29, 30*). We needed to unravel this anomaly, and so we used electrospray mass spectrometry to check the homogeneity of calmodulin. The calmodulin we had isolated from pig brain was essentially homogeneous. The observed molecular mass of 16790.9 Da equals that of bovine brain calmodulin (16790.3 Da) and indicates that the amino acid sequences and post-translational modifications of the pig and bovine calmodulins are identical. Thus truncation in the C-terminal peptide arose because of anomalous trypsin cleavage. It may be that the inhomogeneity in peak 9 arose from peptides related to 127−145, such as 127−148, the peptide found in ref *28*, or 127−144, since C-terminal to Met_{145} is also an anomalous cleavage site (*30*).

Mass Spectrometry of Calmodulin and Its Tryptic Peptides. Electrospray mass spectra of calmodulin were recorded on a VG Platform. Samples were injected through a 10-μL rheodyne loop into a mobile phase of 50% aqueous CH_3CN containing 0.1% (v/v) TFA flowing at 5−20 μL/min into the positive ionization electrospray source. Data were acquired over the appropriate *m*/*z* range, and mass accuracy was ensured by calibration on a separate introduction of horse heart myoglobin (16951.48 Da). FAB mass spectra were

Scheme 1

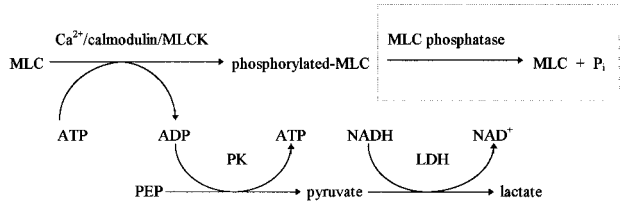

acquired on a VG70-250 SE mass spectrometer in the positive ion mode at an accelerating voltage of 8 kV using a cesium ion gun operating at 20 kV. Approximately 1−10 nmol of sample dissolved in methanol was applied to 2 μL of thioglycerol (Fluka) on the probe tip, and spectra were obtained in continuum mode. Calibration was achieved using 0.5 M CsI/1.0 M NaI (Aldrich Chemical Co.).

Microsequencing of Dansylated Tryptic Peptides. Two peaks (one overlapping with the peak of peptide 31−37) were specific to the tryptic digests of dansyl-calmodulin. They were isolated by HPLC and analyzed by gas-phase microsequencing. Sequence analysis was performed with Applied Biosystems 470A gas-phase and 477A pulsed liquid-phase peptide sequencers. Phenylthiohydantoin-amino acids were analyzed on-line with Applied Biosystems 120A analyzers (*31*). Data collection and analysis were done with an Applied Biosystems 900A module calibrated with 25 pmol of PTH-amino acid standards.

Assay of MLCK Activity. A continuous spectrophotometric assay of MLCK activity was developed on the basis of the measurement of ADP produced by the enzyme reaction. ADP was reconverted to ATP with coupling to NADH oxidation, and the time course of the NADH fluorescence decrease was measured (λ_{ex} = 340 nm, λ_{em} = 460 nm) and quantified by the calibration of the NADH fluorescence. Phosphorylated MLC is a relatively potent product inhibitor of MLCK activity (*32*), but the inhibition could be avoided by one of two ways. At low MLC concentrations (<5 μM), NADH was in excess (40−100 μM) and smooth-muscle MLC phosphatase was added until product inhibition was suppressed. It was also advantageous in that MLC was continuously recycled, extending the range of the assay to cover MLC concentrations below its K_m value (5−14 μM at 30 °C, (*33*)). Alternatively, MLC (typically >10 μM) was in excess of 5 μM NADH, in which case the NADH was used up in the initial stage of the reaction during which product inhibition did not significantly affect the phosphorylation rate. The reactions are summarized in Scheme 1.

Suitable conditions for testing the properties of TA-calmodulin and dansyl-calmodulin in the MLCK assay were first established, for example, by investigating whether MLC phosphatase was required. The K_m of calmodulin and the K_i values of TA-calmodulin and dansyl-calmodulin were then measured as follows. A typical MLCK assay solution contained Ca^{2+}, calmodulin, MLC, MLCK, NADH as required, PK and LDH (Sigma Chemical Co.), 1.2 mM PEP, 500 μM ATP, 2 mM DTT, 50 mM K-MES pH 7.0, 100 mM KCl, and 2 mM $MgCl_2$. Sufficient muscle PK and bovine heart LDH were added for these enzymes not to affect the rate of NADH disappearance. With this assay solution and 120 nM calmodulin, 20 μM MLC, 0.2 nM MLCK (molecular mass: 155 kDa (*34*)), 0.2 mM $CaCl_2$, and 5 μM NADH in 0.5 mL at 22 °C, the specific activity was 12.5 μmol of MLC phosphorylated min^{-1} (mg of MLCK)$^{-1}$. This value compares with 13 μmol min^{-1} mg^{-1} at 25 °C using gizzard MLCK (*35*) and with 8.1 and 8.9 μmol of gizzard and bovine stomach myosin phosphorylated min^{-1} mg^{-1}, respectively, also at 25 °C (*19*).

Phosphodiesterase Activation Assay. PDE activity was determined as a function of calmodulin concentration. The reaction product, AMP, was converted into inosine by a coupled enzyme system, and the rate of adenosine deamination was measured spectrophotometrically (*36*). Calmodulin-deficient PDE, AD, AP, and cyclic AMP were purchased from Boehringer Mannheim. The assay was carried out at 30 °C in 1 mL of 0.1 M glycylglycine·HCl pH 7.5, 3 mM $CaCl_2$, 1.2 mM $MgSO_4$, 90 μM cyclic AMP, AD, AP, and PDE. Amounts of calmodulin, TA-calmodulin or dansyl-calmodulin are specified in Figure 3. Maximum calmodulin activation was set by the rate of PDE-catalyzed hydrolysis of cyclic AMP in the presence of 1 μg/mL calmodulin. The amount of PDE was such that 3 μM inosine was formed per minute. The concentration of inosine was determined from $\epsilon_0 = -8100$ M^{-1} cm^{-1} at 265 nm for adenosine to inosine conversion. Sufficient AD and AP were added for these enzymes not to affect the rate of inosine formation. Stock solutions of calmodulin and labeled calmodulins from which aliquots were taken for the assays contained 1 mg/mL bovine serum albumin. K_m values for native and labeled calmodulins were determined as described below.

Equilibrium, Steady-State Enzyme, and Transient Kinetic Experiments. Unless otherwise stated, all equilibrium, steady-state, and transient kinetic experiments were carried out in 50 mM K-MES pH 7.0, 100 mM KCl, 2 mM $MgCl_2$, and 100 μM $CaCl_2$ at 21 °C. Equilibrium and steady-state measurements of fluorescence were carried out in an SLM Instruments Inc. photon counting fluorimeter. Transient kinetic experiments using TA-calmodulin were carried out as described in ref *13*.

Analysis of Enzyme Kinetics. The kinetic parameters of activator (Figure 3) or inhibitor (Figure 4) calmodulins were determined by a single-substrate Michaelis−Menten model solving the following equations: $v = V_{max}/(1 + K_m/[\text{activator}])$ and $v = V_{max}/\{1 + K_m(1 + [\text{inhibitor}]/K_i)/[\text{activator}]\}$. The program Enzfitter (*37*) was used to obtain best fits to steady-state enzyme activity measurements.

Design and Theory of Peptide Inhibition of MLCK Activity. Two types of measurements were made. First, the calmodulin-activated steady-state MLCK activity was determined in the presence and absence of the peptide inhibitor. From the ratio of the steady-state rates with and without peptide addition, the dissociation constant of the calmodulin−peptide complex was calculated. Second, the steady-state kinase rate was perturbed by the addition of the inhibitor peptide to the assay, and the relaxation to a new steady-state kinase rate was observed. From the exponential process that linked the two steady states, the rate constants that maintain the calmodulin−MLCK complex were calculated.

In observing initial kinase rates the following conditions were adhered to: the concentration of MLCK was negligible compared to the substrates, and the concentrations of the substrates ATP and MLC were sufficiently high not to change significantly in the initial part of the reaction.

Product accumulation was negligible (or could be avoided by using MLC phosphatase, see above).

Calmodulin−MLCK complexes (in equilibrium with ATP and MLC) were assumed to be the active enzyme in steady-state equilibrium with calmodulin and MLCK. The K_m for calmodulin corresponds to the apparent dissociation constant of calmodulin from the prevailing MLCK·substrate (product) steady-state complex (e.g., see Scheme 5). By using this K_m value, it was now possible to measure K_d, the dissociation constant of calmodulin−peptide interactions from the peptide inhibition of MLCK. In the presence of calmodulin and no peptide inhibitor, the steady-state rate of MLCK activity is $v_1 = k_{cat}[cal{\cdot}MLCK]_1$, where $[cal{\cdot}MLCK]_1$ is the concentration of the calmodulin−MLCK steady-state complex. $[cal{\cdot}MLCK]_1$ was determined from $K_m = [cal]_1[MLCK]_1/[cal{\cdot}MLCK]_1$, where $[cal]_1$ and $[MLCK]_1$ are the concentrations of free calmodulin and the relevant MLCK species (e.g., MLCK·MLC-P in Scheme 5), and the K_m for calmodulin (calculated from data in Figure 4) is assumed to correspond to the dissociation constant of calmodulin to MLCK. The velocity of MLCK activity measured in the presence of calmodulin and peptide is $v_2 = k_{cat}[cal{\cdot}MLCK]_2$. $[cal{\cdot}MLCK]_2$, the concentration of the calmodulin−MLCK steady-state complex in the presence of the peptide, was determined from $v_1/v_2 = [cal{\cdot}MLCK]_1/[cal{\cdot}MLCK]_2$.

The concentration of free calmodulin $[cal]_2$ during the measurement of v_2 was determined from $K_m = [cal]_2[MLCK]_2/[cal{\cdot}MLCK]_2$. Knowing $[cal{\cdot}MLCK]_2$ and $[cal]_2$, K_d can be determined:

$$K_d = [cal]_2[peptide]/[cal{\cdot}peptide] = [cal]_2([peptide]_0 - [cal]_0 + [cal]_2 + [cal{\cdot}MLCK]_2)/([cal]_0 - [cal]_2 - [cal{\cdot}MLCK]_2) \quad (1)$$

where concentrations denoted with the 0 subscript are the total concentrations of components.

The rate constants of the calmodulin−MLCK interaction can be determined from the kinetics of re-establishing a steady-state MLCK rate on sequestration of calmodulin by inhibitor peptide (as in Figure 1D). Following the addition of inhibitor peptide during an assay of calmodulin-activated MLCK, the change in the rate of MLCK activity occurs as [cal·MLCK], the concentration of the calmodulin-bound MLCK steady-state complex, decreases:

$$d\,v/d\,t = k_{cat}\,d\,[cal{\cdot}MLCK]/d\,t = k_{cat}\{-k_{-1}[cal{\cdot}MLCK] + k_{+1}[MLCK][cal]\}$$

where

$$cal{\cdot}MLCK \underset{k_{+1}}{\overset{k_{-1}}{\rightleftharpoons}} cal + MLCK$$

assuming the equilibration of sequestered calmodulin with peptide is rapid on the time scale of the assay.

$$d\,[cal{\cdot}MLCK]/d\,t = -k_{-1}[cal{\cdot}MLCK] + k_{+1}[cal]_0([MLCK]_0 - [cal{\cdot}MLCK])/(1 + [peptide]/K_d) = k_{+1}[cal]_0[MLCK]_0/(1 + [peptide]/K_d) - [cal{\cdot}MLCK]\{k_{-1} + k_{+1}[cal]_0/(1 + [peptide]/K_d)\}$$

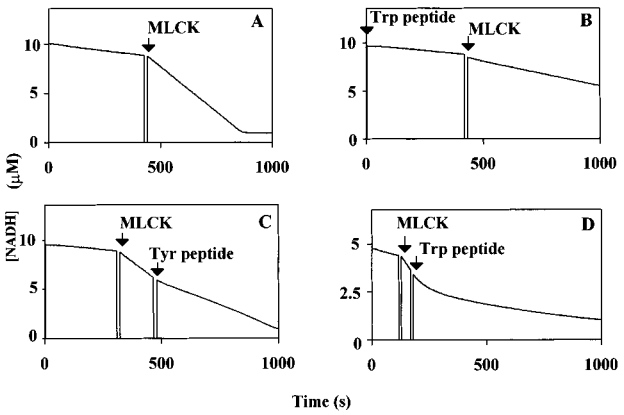

FIGURE 1: Measurement of the inhibition of steady-state MLCK activity by calmodulin binding peptides. Prior to adding MLCK (indicated by arrow), the assay components were allowed to equilibrate until a steady, slow NADH decay was obtained.The MLCK assay mix (0.5 mL) consisted of the following: 50 mM K-MES pH 7.0, 100 mM KCl, 2 mM $MgCl_2$, 100 μM $CaCl_2$, LDH (14 units), PK (13 units), 20 μM MLC, 1.25 mM PEP, ATP as indicated below, 13 μM NADH, 1.5 mM DTT, and 41 nM calmodulin. The assay temperature was 22 °C. Panel A: MLCK activity measurement. ATP concentration was 300 μM. MLCK (0.5 nM) was added to start the reaction. The specific activity of the enzyme was 12.5 μmol of MLC phosphorylated min^{-1} (mg of MLCK)$^{-1}$. Panel B: measurement of K_d of calmodulin for Trp peptide. ATP concentration was 300 μM. The assay mix was equilibrated with 56.1 nM Trp peptide followed by the addition of 36.2 nM MLCK. K_d = 7.1 pM in this experiment. Panel C: measurement of K_d of calmodulin for Tyr peptide. ATP concentration was 100 μM. MLCK (1.44 nM) was added and was followed by 174 nM Tyr peptide. K_d = 7.2 nM in this experiment. Re-equilibration to a new steady state occurred within a few seconds due to the relatively weak binding of Tyr peptide to calmodulin. See text for further analysis. Panel D: displacement of calmodulin from MLCK by Trp peptide. NADH (6.5 μM) was present. ATP concentration was 300 μM. MLCK (0.5 nM) was added followed by 64.6 nM Trp peptide.

As long as [peptide] does not change over the time course of the re-establishment of the MLCK steady-state rate (in practical terms, if $[peptide] \gg [MLCK]_0$), the above equation in [cal·MLCK] has the form of a first-order exponential decay in which the rate constant k_{obs} is given by

$$k_{obs} = k_{-1} + k_{+1}[cal]_0/(1 + [peptide]/K_d) \quad (2)$$

Thus, the measured parameter $d\,v/d\,t$ enabled k_{obs} to be determined as a function of [peptide], from which k_{+1} and k_{-1} may be calculated. If $[peptide] \gg K_d$, as is the case with Trp peptide, $k_{obs} = k_{-1}$. For the above kinetic theory (eq 2) to be valid, k_{obs} must be independent of [Trp peptide].

RESULTS

Steady-State MLCK Assay. The continuous measurement of steady-state kinase activity utilizing the regeneration of ADP was advantageous for assessing both the linearity of the reaction and the relaxation from one steady-state rate to another (Figure 1). A detailed presentation of the data for the determination of the K_m for calmodulin during MLCK activity is left till analysis of the kinetic data of TA-calmodulin and dansyl-calmodulin (Figure 4). These data were also obtained using the ADP/NADH linked assay and show that the K_m of calmodulin was 3.5 nM. Figure 1A shows a typical record at saturating calmodulin. It was

always necessary to allow the assay to run a few minutes before adding MLCK so that an accurate background rate of NADH disappearance was obtained. Another precaution was to measure the rate of NADH disappearance above 2 μM NADH. This is because NADH bound to LDH has a greater fluorescence than NADH alone (*38*), so the rate of fluorescence change associated with the removal of the last of the NADH was as much as 35% greater than it was earlier in the assay. This increased rate is just evident in Figure 1A,C. The K_d of LDH for NADH is 1 μM (*39*).

The other records in Figure 1 illustrate the inhibition by Trp peptide and Tyr peptide of calmodulin-dependent MLCK activity. Thus one inhibition assay yielded two parameters: the dissociation constant of the peptide−calmodulin interaction (K_d) and the dissociation rate constant (k_{-1}) of the calmodulin−MLCK complex in the presence of substrates and 100 μM Ca^{2+}.

Determination of K_d Values of Calmodulin Binding Peptides. In the experiment shown in Figure 1B, Trp peptide in an excess over calmodulin was included in the assay prior to the addition of MLCK. The 72-fold greater concentration of MLCK compared to that shown in Figure 1A is an indication of the high affinity of the peptide for calmodulin. The K_d for the Trp peptide−calmodulin binding was determined from several such assays using eq 1. The K_d value of 8.6 (±1.4) pM is in good agreement with that determined by equilibrium competition with TA-calmodulin from kinetic measurements (Table 1).

A disadvantage of the protocol used in Figure 1B is that the activity of MLCK in the absence of inhibitor peptide had to be measured in a separate assay. This problem was absent when studying inhibition caused by Tyr peptide, which binds much more weakly to calmodulin. A typical record from which K_d was calculated is shown in Figure 1C, and again the K_d value equals that measured in the equilibrium competition experiments (Table 1).

The K_d reported for the peptide RS20 (R-R-K-W-Q-K-T-G-H-A-V-R-A-I-G-R-L-S-S-S) is 1.6 (±0.3) nM (*14*). We used a similar peptide, termed RS20-like peptide (A-R-R-K-W-Q-K-T-G-H-A-V-R-A-I-G-R-L-S-S), and measured K_d values in the range 0.11−0.39 nM as shown in Table 1, consistent with a 10−100-fold weaker binding of calmodulin to RS20-like peptide than to Trp peptide.

Dissociation Rate Constant of the Calmodulin−MLCK Complex in the Presence of Substrates. Figure 1D shows the steady-state MLCK rate and the time course of its decrease on addition of Trp peptide. A single-exponential process with rate constant 0.015 s^{-1} linked the steady-state rates observed before and after inhibitor peptide addition. The inhibition of MLCK by Trp peptide is complete as judged by comparison of the final steady-state rate to that prior to MLCK addition. The observed rate constant of calmodulin displacement changed by less than 20% over the concentration range of 50−800 nM Trp peptide. These data can be interpreted according to eq 2 where k_{obs}, the observed rate constant, is independent of [peptide]. Thus the dissociation rate constant of calmodulin from MLCK in the presence of its substrates, MLC and Mg^{2+}ATP, is k_{-1} = 0.015 s^{-1}. The maximum value of the association rate constant, k_{+1}, will be ~10^8 M^{-1} s^{-1} (i.e., diffusion-controlled and equal to the association rate constant of TA-calmodulin to MLCK (*13*)). Then, under the experimental conditions described in Figure 1D, the right-hand expression in eq 2, $k_{+1}[cal]_0/(1 + [peptide]/K_d) = 4.1K_d/[peptide]$. At 50 nM Trp peptide and 41 nM calmodulin, [peptide] = 9 nM so that $4.1K_d/[peptide] = 0.004$ s^{-1}. This is consistent with the low sensitivity of k_{obs} to Trp peptide concentration since, even at the lowest concentration of Trp peptide, k_{obs} would be at most 26% greater than k_{-1}. In contrast to Trp peptide, inhibition by Tyr peptide occurred within 10 s (i.e., at >0.07 s^{-1}) (Figure 1C). From eq 2, $k_{obs} = 0.20$ s^{-1} [taking k_{-1} = 0.015 s^{-1}, $k_{+1} = 10^8$ M^{-1} s^{-1}, $[cal]_0$ = 41 nM, K_d = 7.2 nM, and [peptide] = 155 nM (corrected for Tyr peptide bound to calmodulin)], which is also consistent with the observed rate of the onset of Tyr peptide inhibition.

Kinetic Mechanism of RS20-Like Peptide and TA-Calmodulin Interaction. RS20-like peptide is an analogue of Trp peptide. Trp peptide is acetylated at the N terminus and amidated at the C terminus. In contrast, RS20-like peptide has free N and C termini. Given the much weaker affinities of RS20 (Table 1) and the RS20-like peptide (measured above), it was of interest to find out the mechanistic basis of this difference.

Association Kinetics of TA-Calmodulin and RS20-Like Peptide. The fluorescence transients shown in Figure 2A,B were obtained when 11 nM TA-calmodulin and 45 nM RS20-like peptide were rapidly mixed. The secondary plot shown in Figure 2C was derived by varying the concentration of the RS20-like peptide. The solvent and temperature were as specified in Materials and Methods.

The biphasic kinetics with the RS20-like peptide were reminiscent of that observed with Trp peptide and Tyr peptide in ref *13*. We modeled the mechanism of interaction of the RS20-like peptide by Scheme 2, a two-step mechanism that was consistent with the interaction of Trp and Tyr peptides with TA-calmodulin (*13*).

F_1, F_2, and F_3 represent the relative fluorescence of TA-cal, TA-cal·RS20-like peptide, and TA-cal·RS20-like peptide*, respectively. F_1 was defined as 1 and, from the records in Figure 2A,B, $F_2 = 1.9$. The fluorescence intensity at the end of the reaction was $F_\infty = 1.7$ (Figure 2B). In terms of Scheme 2, the following rate constants were determined: k'_{+1} = 9.14 (±1.02) × 10^8 M^{-1} s^{-1} (gradient of k'_{obs} as a function of peptide concentration, Figure 2C) and $k'_{+2} + k'_{-2} = 0.98$ (±0.045) s^{-1} (mean of k'^*_{obs}, Figure 2C).

Dissociation Kinetics of TA-cal·RS20-Like Peptide Complex. The dissociation kinetics of RS20-like peptide from TA-calmodulin were measured by mixing the binary complex with excess calmodulin so that the latter trapped the RS20-like peptide as it dissociated. Thus 1 μM calmodulin was rapidly mixed with the equilibrated mixture of 11 nM TA-calmodulin and 45 nM RS20-like peptide (mixing chamber concentrations). TA-calmodulin dissociation was biphasic; the fluorescence decay is shown in Figure 2D. The theory developed in ref *13* was applied to the analysis of these kinetic data in terms of Scheme 3.

The best fit to two exponentials of TA-calmodulin dissociation gave $\lambda_1 = 2.25$ (±1.70) s^{-1} and $\lambda_2 = 0.24$ (±0.04) s^{-1} with amplitude ratio $\Lambda_1/\Lambda_2 = 0.35$. In terms of Scheme 2, λ_1 and λ_2 are the roots of the equation $\lambda^2 - (k'_{-1} + k'_{+2} + k'_{-2})\lambda + k'_{-1}k'_{-2} = 0$, from which $\lambda_1 + \lambda_2 = k'_{-1} + k'_{+2} + k'_{-2}$ and $\lambda_1\lambda_2 = k'_{-1}\,k'_{-2}$. The constraint $k'_{+2} + k'_{-2}$ = 0.98 s^{-1} (Figure 2C) leads to $k'_{-1} = 1.51$ s^{-1}; $k'_{+2} = 0.63$

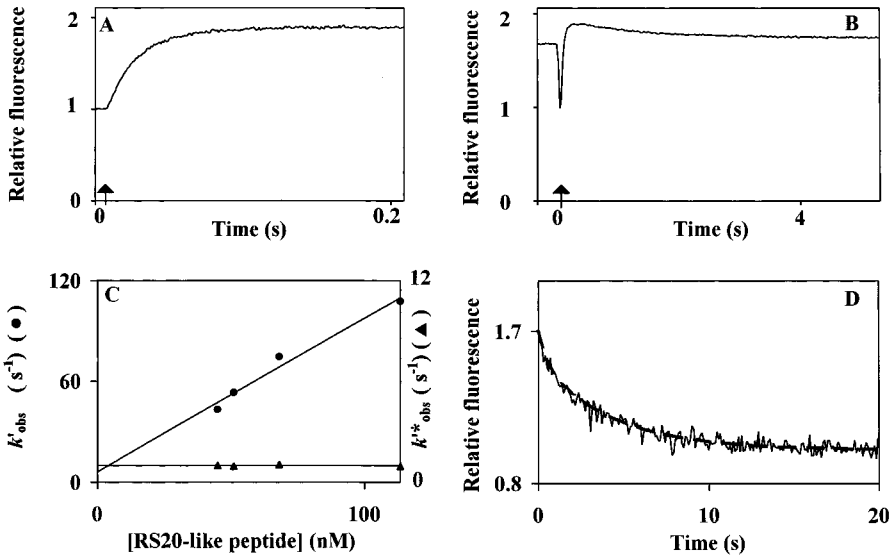

FIGURE 2: Association and dissociation kinetics of TA-calmodulin and RS20-like peptide. In panels A and B, fluorescence transients were obtained by rapid mixing of 11 nM TA-calmodulin and 45 nM RS20-like peptide (concentrations in the mixing chamber) in a stopped-flow fluorimeter (λ_{ex} = 365 nm, λ_{em} > 400 nm) as described in Materials and Methods. Time 0 (marked by the arrows) is defined by stopping the flow of solutions. In panel A, the fluorescence of the solutions flowing is shown prior to time 0. In panel B, the fluorescence of the end-of-reaction mixture precedes that of the fluorescence during flow prior to time 0. In panel C, the rate constants of the two exponential phases of the reaction were plotted as a function of [RS20-like peptide]. k'_{obs} denoted values for the fast phase and k'^*_{obs} for the slow phase. The gradient of the linear regression line for the data (●) was 9.14 (±1.02) × 10^8 M^{-1} s^{-1} (k'_{+1} in Scheme 4), and the intercept was 6.35 (±0.74) s^{-1}. Values for k'^*_{obs} were fitted with a horizontal line at 0.98 (±0.05) s^{-1} ($k'_{+2} + k'_{-2}$ in eq 2). In panel D, TA-calmodulin was displaced from RS20-like peptide by calmodulin. Calmodulin (1 μM) was rapidly mixed with the equilibrated mixture of 11 nM TA-calmodulin and 45 nM RS20-like peptide (mixing chamber concentrations). This record was taken at a reduced excitation slit width and increased photomultiplier sensitivity to counter photobleaching, hence the noise on the data. Nonlinear least-squares fitting to two exponentials of amplitude Λ_1 and Λ_2 and rate constants λ_1 and λ_2 (eq 8 in Török and Trentham, 1994) gave λ_1 = 2.25 (±1.70) s^{-1} and λ_2 = 0.24 (±0.04) s^{-1}. The amplitude ratio was Λ_1/Λ_2 = 0.35 (±0.07). The line overlaying the data was generated by using the following parameters: k'_{-1} = 1.51 s^{-1}, k'_{+2} = 0.63 s^{-1}, k'_{-2} = 0.36 s^{-1}, F_1 = 1, F_2 = 1.9, and F_3 = 1.6. The calculated amplitude ratio for these values was 0.30.

Scheme 2

$$\underset{F_1}{\text{TA-cal + RS20-like peptide}} \underset{k'_{-1}}{\overset{k'_{+1}}{\rightleftharpoons}} \underset{F_2}{\text{TA-cal.RS20-like peptide}} \underset{k'_{-2}}{\overset{k'_{+2}}{\rightleftharpoons}} \underset{F_3}{\text{TA-cal.RS20-like peptide*}}$$

Scheme 3

$$\text{TA-cal.RS20-like peptide*} \underset{k'_{+2}}{\overset{k'_{-2}}{\rightleftharpoons}} \text{TA-cal.RS20-like peptide} \overset{k'_{-1}}{\rightleftharpoons} \text{TA-cal + RS20-like peptide}$$

$$\searrow$$

peptide trapped by calmodulin

Scheme 4

$$\underset{F_1 = 1}{\text{TA-cal + RS20-like peptide}} \overset{9.14 \times 10^8\ M^{-1}s^{-1}}{\underset{1.51\ s^{-1}}{\rightleftharpoons}} \underset{F_2 = 1.9}{\text{TA-cal.RS20-like peptide}} \overset{0.63\ s^{-1}}{\underset{0.36\ s^{-1}}{\rightleftharpoons}} \underset{F_3 = 1.59}{\text{TA-cal.RS20-like peptide*}}$$

s^{-1}; and k'_{-2} = 0.36 s^{-1}. Now using all the data in Figure 2, $K'_d = k'_{-1}k'_{-2}/k'_{+1}(k'_{+2} + k'_{-2})$ = 0.60 nM. F_3 = 1.59 and is derived from a knowledge of F_∞, F_2, k'_{+2}, and k'_{-2}. These values can be fed back into eq 10 of ref *13* to determine Λ_1/Λ_2 = 0.30 in good agreement with Λ_1/Λ_2 = 0.35 measured experimentally in Figure 2D. All of these results can be summarized by putting the appropriate values into Scheme 2.

As seen in Figure 2D, the calculated values of the parameters of the above reaction (Scheme 4) gave a good fit for the data. However, there was a large error in λ_1 = 2.25 (±1.70) s^{-1}, so the range of the estimates was determined: the lower limit $\lambda_1 + \lambda_2$ = 0.76 s^{-1} was taken to satisfy the requirement for $\lambda_1 + \lambda_2 \geq k'_{+2} + k'_{-2}$. k'_{-2} was limited by $F_3 > 0$, and that gave $k'_{-2} < 0.88$ s^{-1}. With these considerations, the range of values was $0 < F_3 < 1.6$, 0.23 $s^{-1} < k'_{-1} < 4.0$ s^{-1}, 0.37 $s^{-1} < k'_{-2} < 0.88$ s^{-1}, 0.10 $s^{-1} < k'_{+2} < 0.61$ s^{-1}, and 0.23 nM < K'_d < 1.6 nM.

In summary, RS20-like peptide interacted with TA-calmodulin in a similar way to that seen with Tyr and Trp peptides. A biphasic fluorescence change occurred in the association of RS20-like peptide with TA-calmodulin, the first phase of which represented a bimolecular reaction, and the second phase was concentration independent. The formation of the initial TA-calmodulin−peptide complex was rapid and diffusion-limited. Isomerization of this complex occurred at 1 s^{-1}. The dissociation of the equilibrated complex was biphasic and thus allowed estimates of other parameters of the interaction. The bimolecular association rate constants of all three peptides were essentially the same and indicated diffusion-controlled complex formation between the peptide and calmodulin. Likewise all three peptides and MLCK (*13*) underwent an isomerization following binary complex formation. Differences in the dissociation constants arose from differences in the kinetics of dissociation, in particular in k'_{-1}.

Dissociation Constants of Calmodulin for RS20-Like Peptide and Control E_4E_{17} Peptide for Calmodulin. Dissociation constants of targets for calmodulin are conveniently determined by equilibrium competition assay with TA-calmodulin. Typically K_d values for calmodulin are 0.4-fold those for TA-calmodulin (*13*). In the case of RS20-like peptide however, this assay gave a complex result, possibly indicative of binding of two peptide molecules to calmodulin with a 10-fold difference in K_d values (data not shown). Therefore, in contrast to the situation with Trp peptide (*13*), it was not possible to combine the kinetic analysis of the RS20-like peptide interaction with TA-calmodulin and the competition assay to calculate the K_d of RS20-like peptide

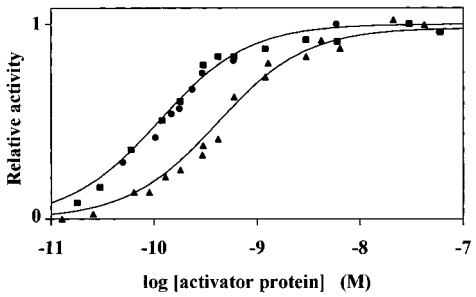

FIGURE 3: Activation of PDE by calmodulin, TA-calmodulin, and dansyl-calmodulin. Activity of PDE relative to that in the presence of 1 μg/mL calmodulin was measured in the presence of calmodulin (■), TA-calmodulin (▲) and dansyl-calmodulin (●) under assay conditions described in Materials and Methods. The solid lines represent the best fit to Michaelis−Menten kinetics for calmodulin (left-hand line) and TA-calmodulin (right-hand line).

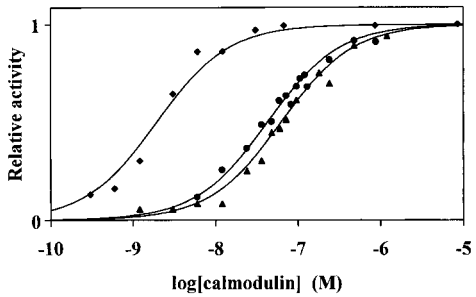

FIGURE 4: Inhibition of MLCK by TA-calmodulin and dansyl-calmodulin. The concentration of MLCK was 0.2 nM and of ATP was 0.5 mM. Specific activity of MLCK was measured in the presence of calmodulin (◆) under the typical MLCK assay conditions described in Materials and Methods. Inhibition of MLCK with respect to calmodulin in the presence of 235 nM TA-calmodulin (▲), or 235 nM dansyl-calmodulin (●) is shown. The curves represent best fits to Michaelis−Menten kinetics treating calmodulin as the activator protein and TA-calmodulin and dansyl-calmodulin as competitive inhibitors. K_m was fitted to the theory of single substrate activation in Michaelis−Menten kinetics. Note that a steeper dependence on calmodulin concentration would give a better fit, suggesting cooperativity in the process.

with calmodulin directly. However, on the basis of the 0.4-fold ratio of K_d values between calmodulin and TA-calmodulin, we estimated that the K_d value of calmodulin and the RS20-like peptide is 0.09−0.64 nM. This value is within the range determined by the MLCK inhibition assay (see Table 1). Thus RS20-like peptide binds 10−100-fold more weakly to calmodulin and TA-calmodulin than does Trp peptide.

For tests of binding specificity, the control peptide, the E_4E_{17} analogue of Trp peptide, was designed. This peptide contains two negatively charged groups in place of Trp and Leu at residues 4 and 17, respectively. Predictably, the K_d of the control peptide to TA-calmodulin was 11.8 μM, 10^6-fold greater than that of the Trp peptide. Thus K_d of the control peptide for calmodulin was estimated to be 4.7 μM (Table 1).

Preparation of Specifically Labeled Dansyl-Calmodulin and Identification of the Labeling Site. We expected Lys_{75}-dansylated calmodulin (dansyl-calmodulin) to be the main derivative if dansylation of calmodulin is carried out in the same conditions as labeling with TA-Cl (*13*). The labeling site in dansyl-calmodulin was determined by isolating and identifying dansylated peptides in the tryptic digest of dansyl-calmodulin. Dansylated peptides were indicated by the differences in the HPLC elution profiles of calmodulin and dansyl-calmodulin digests. The peak representing the Lys_{75}−Arg_{86} peptide was absent following dansylation. Gas-phase microsequencing of a new peptide peak immediately following that containing peptide 31−37 gave the sequence Xaa-Met-Lys-Asp-, suggesting that this peak corresponded to the modified Lys_{75}−Arg_{86} peptide. When the material of the peak of peptide 31−37 was sequenced, it contained not only the expected amino acids but also an additional component that sequenced as Xaa-Met-, suggesting a further Lys_{75}-modified peptide, most probably ϵ-dansyl-Lys_{75}-Met-Lys_{77}. These data are consistent with Lys_{75} being the sole labeled amino acid in dansyl-calmodulin. The biological properties of dansyl-calmodulin purified to homogeneity were tested alongside with those of TA-calmodulin (see below).

Modulation of Enzyme Activity by TA-Calmodulin and Dansyl-Calmodulin. PDE activation by TA-calmodulin and dansyl-calmodulin is shown in Figure 3. TA-calmodulin activated PDE with a 3.5-fold greater K_m but to the same V_{max} as the unlabeled calmodulin. The K_m for calmodulin was 0.13 (±0.025) nM and 0.45 (±0.17) nM for TA-calmodulin. Dansyl-calmodulin activated PDE with a K_m of 0.13 nM, a value indistinguishable from that for calmodulin.

In contrast, neither TA-calmodulin nor dansyl-calmodulin was an activator of MLCK. The Ca^{2+}-calmodulin-dependent activity was competitively inhibited by TA-calmodulin with $K_i/K_m = 3.6$ (±0.44 sd) and by dansyl-calmodulin with $K_i/K_m = 5.6$ (Figure 4). The K_m for calmodulin was 3.5 nM.

To test for possible contamination of calmodulin in TA-calmodulin, an assay under the conditions described in Materials and Methods was carried out in the presence of 600 nM TA-calmodulin but no added calmodulin. If TA-calmodulin had been contaminated by 1% calmodulin (i.e., 6 nM), then on the basis of the data derived from Figure 4 (see previous paragraph), the specific activity would have been 0.3 μmol of MLC phosphorylated min^{-1} (mg of MLCK)$^{-1}$, and well above the observed specific activity that was <0.1 μmol min^{-1} (mg of MLCK)$^{-1}$. Thus we conclude that the contamination of TA-calmodulin by calmodulin was <1%. These data also show that DET-calmodulin is not an activator of MLCK and suggest that, like TA-calmodulin, DET-calmodulin is substituted at Lys_{75}.

DISCUSSION

Trp peptide and the peptide termed RS20 (*14*) only differ at their termini: Trp peptide is 3 amino acids shorter and its termini are blocked. Yet their reported K_d values to calmodulin in the presence of Ca^{2+} differ over 100-fold. We checked using an independent method, a continuous steady-state MLCK activity assay, the K_d values of calmodulin to Trp, Tyr, and RS20-like peptides and determined the K_d of RS20-like peptide by transient kinetic methods using TA-calmodulin. The results confirmed both the original K_d estimates for Trp and Tyr peptides and the 1−2 orders of magnitude difference between these and RS20-like peptide. The E_4E_{17} homologue of Trp peptide bound TA-calmodulin with a 10^6-fold higher K_d (10 μM) and inhibited MLCK activity negligibly. This peptide is thus a useful control for the specificity of Trp peptide function. The tight binding of Trp peptide (6 pM) makes it suitable for displacing

calmodulin bound to target proteins both in vitro and in vivo (*2*). There are two issues to consider when using calmodulin inhibitors. These are illustrated in Figure 1, panels C and D by the examples of Tyr peptide and Trp peptide, respectively. Tyr peptide causes partial inhibition, and re-equilibration occurs within a few seconds. In contrast, inhibition of MLCK activity by Trp peptide is complete and takes several minutes. These differences arise from the K_d values of these peptides to calmodulin. Trp peptide efficiently traps calmodulin. The result of this is that the free calmodulin concentration is very low, so calmodulin rebinding to MLCK is negligible. Thus inhibition sets in at the rate of calmodulin dissociation from MLCK. When Trp peptide is applied in physiological systems, the slow time course of calmodulin dissociation (shown in Figure 1D for MLCK) from target enzymes has to be taken into account when Ca^{2+} is present at or above Ca^{2+} activation levels. It is noteworthy that Trp peptide, when injected into sea urchin egg prior to fertilization (i.e., at low Ca^{2+}), was fully effective in preventing mitotic transitions following fertilization (*2*). In contrast, Tyr peptide, whose affinity for calmodulin is comparable to that of MLCK, is a less efficient trap for calmodulin (Figure 1C).

RS20-like peptide interacted with TA-calmodulin in a manner similar to that of the Trp and Tyr peptides: biphasic fluorescence changes occurred both on association and dissociation. Diffusion-limited association was followed by an isomerization at 1 s^{-1}. The weaker binding of the RS20-like peptide to calmodulin was dependent on a more rapid dissociation rate constant from the protein and may be due to the charged amino and carboxylate groups at either end of the peptide. Consistent with the data showing an isomerization is the abundant kinetic evidence of the conformational changes when calmodulin interacts with target peptides (*13*, *40*−*42*).

Calmodulin has been covalently modified with a fluorescent Lys reagent, TA-Cl, with the aim of producing specifically labeled derivatives that respond to Ca^{2+} and target protein (peptide) binding with fluorescence changes in the presence of physiological concentrations of K^+ and Mg^{2+}. The sensitivity of the fluorescence signal allowed mechanistic studies of TA-calmodulin and of its interactions with Ca^{2+} and target proteins and peptides in the nanomolar concentration range. Lys_{75}-modified dansyl-calmodulin was made and purified similarly to TA-calmodulin. Unlike commercially available material, it was a homogeneous protein and therefore suitable for biochemical assays. The properties of the fluorescent calmodulins are interesting from a structural point of view and relevant to their use as probes of cellular function. Lys_{75} is located in the central helix of calmodulin. In Ca^{2+}-calmodulin, residues 78−81 which form part of the central helix in the crystal structure (*43*) are nonhelical in solution (*44*). In the complex with the calmodulin binding peptide of skeletal myosin light-chain kinase, a flexible loop was identified between residues 74 and 82 (*45*). Since Lys_{75} is found in the region of calmodulin that undergoes the most substantial structural changes upon target binding, a probe attached to this site is well positioned to report these structural changes.

Binding to and activation of target proteins are the normal functions of calmodulin. Covalent modification of Lys_{75} may help resolve structural aspects of these two functions. TA-calmodulin and dansyl-calmodulin have been shown here to be activators of PDE with an increased K_m relative to calmodulin and competitive inhibitors of calmodulin with respect to MLCK activation. Results with MLCK show how complicated the situation may be. Thus our results are similar to those obtained in ref *46* when labeling Lys_{75} with norchlorpromazine isothiocyanate. On the other hand calmodulin was also labeled with a fluorescent isothiocyanate under similar conditions, and so possibly at Lys_{75}, but in that case the labeled calmodulin activated MLCK (*47*). It may be that in this case the *N*,*N*-dimethyl-bis-(*N*-1,3-propylidene)ammonium group that interposes the tetramethine-merocyanine and putative Lys_{75} permits the activation by reducing steric interference and/or preserving the positive charge associated with Lys_{75} prior to its modification. However, in the light of our results with TA-calmodulin and dansyl-calmodulin, labeling with the isothiocyanate may have been incomplete at Lys_{75} so that MLCK activation was due to residual native calmodulin.

The enzyme kinetic results suggest that Lys_{75}-modified calmodulins bind to target proteins with comparable affinity to calmodulin, but with different consequences for the target protein activity, a particular derivative can act as either agonist or antagonist (*48*). TA-calmodulin appears to be the first to distinguish between PDE and MLCK, being an agonist to the former and an antagonist to the latter. Small-angle X-ray scattering data have revealed how calmodulin can interact with target peptides in distinct modes (*49*, *50*). Atomic resolution X-ray structures also reveal the diversity that the central helix of calmodulin exhibits when calmodulin interacts with target peptides (*51*). Finally the conformation taken up by calmodulin on binding to MLCK has been shown by energy transfer to be different from that on its binding to PDE (*52*). Thus our kinetic data fit into the pattern of these structural results.

Scheme 5

$$\begin{array}{ccc} \text{cal} + \text{MLCK.MLC-P} & & \\ \quad K_m \uparrow\downarrow & & \\ \text{cal.MLCK.MLC-P} & \xrightarrow{k_{cat}} & \text{cal.MLCK} + \text{MLC-P} \end{array}$$

We now address the 18-fold difference between the K_m of calmodulin as an activator of MLCK activity and the dissociation constant of the calmodulin MLCK interaction. Let us suppose for the purpose of argument that the association rate constants of ADP with MLCK·MLC-P and cal·MLCK.MLC-P are rapid, that ADP binds weakly to these complexes, and that MLC-P release is the rate-limiting step of calmodulin-activated MLCK activity. Then the critical steps defining the K_m of calmodulin during MLCK activity can be represented by Scheme 5, and the rate of MLC−P formation, ν, is given by

$$\nu = k_{cat}[\text{cal·MLCK·MLC-P}]$$

Let us further suppose that $[\text{cal}]_0 \gg [\text{MLCK}]_0$, then

$$\nu = k_{cat}[\text{MLCK}]_0/(1 + K_m/[\text{cal}])$$

where K_m, the measured Michaelis constant, is also the dissociation constant of the calmodulin MLCK·MLC-P interaction. Thus in this model, product dissociation is rate-limiting and K_m = 3.5 nM. The thermodynamics of the

Scheme 6

$$\begin{array}{ccc} & K_d' & \\ \text{MLC-P + cal + MLCK} & \rightleftharpoons & \text{cal + MLCK.MLC-P} \\ 0.2\ \text{nM} \Downarrow (K_d) & & (K_m) \Downarrow 3.5\ \text{nM} \\ & K_d'' & \\ \text{MLC-P + cal.MLCK} & \rightleftharpoons & \text{cal.MLCK.MLC-P} \end{array}$$

Scheme 7

$$\begin{array}{l} \text{cal + MLCK.MLC.ATP} \\ \quad K_m \Downarrow \\ \text{cal.MLCK.MLC.ATP} \xrightarrow{k_{cat}} \text{ADP + cal.MLCK.MLC-P} \xrightarrow{\text{rapid}} \text{cal.MLCK} \\ \qquad\qquad\qquad\qquad\qquad\qquad\qquad\qquad\qquad\qquad + \text{MLC-P} \end{array}$$

interaction of calmodulin, MLCK, and MLC-P is represented by Scheme 6, where $K_d' = [\text{MLC-P}][\text{MLCK}]/[\text{MLCK·MLC-P}]$ and $K_d'' = [\text{MLC-P}][\text{cal·MLCK}]/[\text{cal·MLCK·MLC-P}]$. This leads to $K_d''/K_d' = 3.5/0.2 = 18$; that is, MLC-P binds 18-fold more tightly to MLCK than it does to cal·MLCK. A kinetic implication is that calmodulin promotes MLC-P release, a plausible explanation of the observed phenomena.

Let us now consider an alternative mechanism in which the rate-limiting step is the transfer of the phosphate group to MLC, and ATP saturates MLCK and the cal·MLCK, MLCK·MLC, and cal·MLCK·MLC complexes with equal affinity. Now the critical steps defining the K_m of calmodulin during MLCK activity can be represented by Scheme 7. Then comparable logic to the above analysis of Schemes 5 and 6 leads to the conclusion that MLC binds 18-fold more tightly to MLCK than to cal·MLCK. This is an unlikely though not impossible mechanism so we consider Scheme 5 to be more likely than Scheme 7.

However, more research is needed to define a calmodulin-dependent MLCK mechanism which must also accommodate evidence suggesting that a primary role of calmodulin is to sequester an inhibitory peptide within the MLCK sequence away from the kinase active site. To be specific, a mechanism for calmodulin activation of MLCK has been proposed in which calmodulin binds to a region of a pseudosubstrate domain of MLCK that has autoinhibitory properties (*53*, *54*, and references in each). The calmodulin binding causes the inhibition to be removed by exposing the substrate binding site. The hypothesis requires modification in the light of the catalytic behavior of mutant forms of MLCK and their tryptic digests (*55*). Furthermore, while our data do not invalidate the pseudosubstrate domain model, the existence of inhibitory calmodulin derivatives, such as TA-calmodulin and dansyl-calmodulin, suggests that activation by calmodulin may involve additional structural changes in the calmodulin−MLCK complex. It is noteworthy that the K_i value for TA-calmodulin and MLCK (Figure 4) is 27−59-fold greater than its K_d (0.23−0.51 nM, (*13*)). This ratio is comparable to the K_m/K_d of calmodulin and MLCK and is consistent with TA-calmodulin binding to the same MLCK complex as calmodulin (e.g., MLCK·MLC-P in Scheme 5).

Finally, the sensitivity of the fluorescence signal, especially with respect to Ca^{2+} binding means that TA-calmodulin may complement other intracellular calmodulin imaging probes (*2*, *4*, *9*). Dansyl-calmodulin is more likely to be of value in noncellular systems, since the near-UV irradiation required for its excitation is likely to cause cellular damage and because cells autofluoresce in the same wavelength range. Both Lys_{75}-labeled calmodulins could have contrasting effects as compared to calmodulin target peptides; the labeled calmodulins will only inhibit some target enzymes as opposed to the indiscriminate inhibitory effect of the target peptides on calmodulin-dependent enzymes. For example, in smooth muscle cells one would expect the peptides to inhibit all processes stimulated by calmodulin, while Lys_{75}-labeled calmodulins, though inhibiting MLCK, may promote the activity of other calmodulin-dependent enzymes. The commercial availability of dansyl-chloride means that a Lys_{75}-labeled calmodulin is readily prepared for such studies.

REFERENCES

1. Rasmussen, C. D., and Means, A. R. (1989) *Trends Neurosci. 12*, 433−438.
2. Török, K., Wilding, M., Patel, R., and Whitaker, M. J. (1995) *Biophys. J. 68*, A228.
3. Wilding, M., Török, K., and Whitaker, M. J. (1995) *Zygote 3*, 219−224.
4. Zimprich, F., Török, K., and Bolsover, S. R. (1995) *Cell Calcium 17*, 233−238.
5. Lorca, T., Galas, S., Fesquet, D., Devault, A., Cavadore, J.-C., and Doree, M. (1991) *EMBO J. 10*, 2087−2093.
6. Itoh, T., Ikebe, M., Kargacin, G. J., Hartshorne, D. J., Kemp, B. E., and Fay, F. S. (1989) *Nature 338*, 164−167.
7. Kargacin, G. J., Ikebe, M., and Fay, F. S. (1990) *Am. J. Physiol. 259*, C315−C324.
8. McCarron, J. G., McGeown, J. G., Reaedon, S., Ikebe, M., Fay, F. S., and Walsh, J. V., Jr. (1992) *Nature 357*, 74−77.
9. Hahn, K. M., De Biasio, R., and Taylor, D. L. (1992) *Nature 359*, 736−738.
10. Gough, A. H., and Taylor, D. L. (1993) *J. Cell Biol. 121*, 1095−1108.
11. Fay, F. S., Gilbert, S. H., Drummond, R. M., Ikebe, M., and Walker, J. W. (1997) *Biophys. J. 72*, A236.
12. Miyawaki, A., Llopis, J., Heim, R., McCaffery, J. M., Adams, J. A., Ikura, M., and Tsien, R. Y. (1997) *Nature 388*, 882−887.
13. Török, K., and Trentham, D. R. (1994) *Biochemistry 33*, 12807−12820.
14. Lukas, T. J., Burgess, W. H., Prendergast, F. G., Lau, W., and Watterson, D. M. (1986) *Biochemistry 25*, 1458−1464.
15. Kincaid, R. L., Vaughan, M., Osborne, J. C., Jr., and Tkachuk, V. A. (1982) *J. Biol. Chem. 257*, 10638−10643.
16. Török, K., Lane, A. N., Martin, S. R., Janot, J.-M., and Bayley, P. M. (1992) *Biochemistry 31*, 3452−3462.
17. Cowley, D. J., O'Kane, E., and Todd, R. S. (1991) *J. Chem. Soc., Perkin Trans. 2*, 918−923.
18. Golesworthy, R. C., Shaw, R. A., and Smith, B. C. (1962) *J. Chem. Soc.* 1507−1508.
19. Walsh, M. P., Hinkins, S., Flink, I. L., and Hartshorne, D. J. (1982) *Biochemistry 21*, 6890−6896.
20. Ikebe, M., Stepinska, M., Kemp, B. E., Means, A. R., and Hartshorne, D. J. (1987) *J. Biol. Chem. 262*, 13828−13834.
21. Laemmli, U. K. (1970) *Nature 227*, 680−685.
22. Marston, S. B., Redwood, C. S., and Leyman, W. (1988) *Biochem. Biophys. Res. Commun. 155*, 197−202.
23. Hathaway, D. R., and Haeberle, J. R. (1983) *Anal. Biochem. 135*, 37−43.
24. Alessi, D., Macdougall, L. K., Sola, M. M., Ikebe, M., and Cohen, P. (1992) *Eur. J. Biochem. 270*, 1023−1035.
25. Klee, C. B. (1977) *Biochemistry 16*, 1017−1024.
26. Bradford, M. M. (1976) *Anal. Biochem. 72*, 248−254.
27. Gill, S. C., and von Hippel, P. H. (1989) *Anal. Biochem. 182*, 319−326.
28. Newton, D. L., and Klee, C. B. (1989) *Biochemistry 28*, 3750−3757.
29. Faust, F. M., Slisz, M., and Jarrett, H. W. (1987) *J. Biol. Chem. 262*, 1938−1941.

30. Watterson, D. M., Sharief, F., and Vanaman, T. C. (1980) *J. Biol. Chem. 255,* 962−975.
31. Geisow, M. J., and Aitken, A. (1989) in *Protein Sequencing: A Practical Approach* (Findlay, J. B. C., and Geisow, M. J., Eds.) pp 85−98, IRL Press, Oxford.
32. Sobieszek, A. (1985) *Biochemistry 24,* 1266−1274.
33. Stull, J. T., Nunnally, M. H., and Michnoff, C. H. (1986) in *The Enzymes* (Boyer, P. B., and Krebs, E. G., Eds.) 3rd ed., Vol. 17, pp 113−166, Academic Press, Inc., New York.
34. Gallagher, P. J., Herring, B. P., Griffin, S. A., and Stull, J. T. (1991) *J. Biol. Chem. 266,* 23936−23944.
35. Ikebe, M., and Hartshorne, D. J. (1986) *J. Biol. Chem. 261,* 8249−8253.
36. Schiefer, S. (1985) in *Methods of Enzymatic Analysis* (Bergmeyer, H. U., Ed.) 3rd ed., Vol. 9, pp 317−331, VCH, Weinheim.
37. Leatherbarrow, R. J. (1987) *Enzfitter for IBM PC,* Elsevier-Biosoft.
38. Velick, S. F. (1958) *J. Biol. Chem. 233,* 1455−1467.
39. Stinson, R. A., and Holbrook, J. J. (1973) *Biochem. J. 131,* 719−728.
40. Bowman, B. F., Peterson, J. A., and Stull, J. T. (1992) *J. Biol. Chem. 267,* 5346−5354.
41. Johnson, J. D., Holroyde, M. J., Crouch, T. H., Solaro, R. J., and Potter, J. D. (1981) *J. Biol. Chem. 256,* 12194−12198.
42. Montigiani, S., Neri, G., Neri, P., and Neri, D. (1996) *J. Mol. Biol. 258,* 6−13.
43. Babu, Y. S., Bugg, C. E., and Cook, W. J. (1988) *J. Mol. Biol. 204,* 191−204.
44. Ikura, M., Spera, S., Barbato, G., Kay, L. E., Krinks, M., and Bax, A. (1991) *Biochemistry 30,* 9216−9228.
45. Ikura, M., Clore, G. M., Gronenborn, A. M., Zhu, G., Klee, C. B., and Bax, A. (1992) *Science 56,* 632−638.
46. Newton, D. L., and Klee, C. B. (1984) *FEBS Lett. 165,* 269−272.
47. Hahn, K. M., Waggoner, A. S., and Taylor, D. L. (1990) *J. Biol. Chem. 265,* 20335−20345.
48. Klee, C. B. (1988) Molecular Aspects of Cellular Regulation in *Calmodulin* (Cohen, P., and Klee, C. B., Eds) pp 35−56, Vol. 5, Elsevier, New York.
49. Kataoka, M., Head, J. F., Vorherr, T., Krebs, J., and Carafoli, E. (1991) *Biochemistry 30,* 6247−6251.
50. Trewhella, J., Blumenthal, D. K., Rokop, S. E., and Seeger, P. A. (1990) *Biochemistry 29,* 9316−9324.
51. Meador, W. E., Means, A. R., and Quiocho, F. A. (1993) *Science 262,* 1718−1721.
52. O'Hara, P. B., Grabarek, Z., Mabuchi, Y., Macek, V. J., Pianka, G. A., and Hallert, G. E. (1994) *Biophys. J. 66,* A58.
53. Fitzsimons, D. P., Herring, B. P., Stull, J. T., and Gallagher, P. J. (1992) *J. Biol. Chem. 267,* 23903−23909.
54. Knighton, D. R., Pearson, R. B., Sowadski, J. M., Means, A. R., Ten Eyck, L. F., Taylor, S. S., and Kemp, B. E. (1992) *Science 258,* 130−135.
55. Yano, K., Araki, Y., Hales, S. J., Tanaka, M., and Ikebe, M. (1993) *Biochemistry 32,* 12054−12061.

BI972773E